

Cell type-specific aspects in biocompatibility testing: the intercellular contact in vitro as an indicator for endothelial cell compatibility

Kirsten Peters · Ronald E. Unger · Susanne Stumpf · Julia Schäfer · Roman Tsaryk · Bettina Hoffmann · Eva Eisenbarth · Jürgen Brems · Günter Ziegler · C. James Kirkpatrick

Received: 18 July 2006 / Accepted: 27 October 2006 / Published online: 4 October 2007
© Springer Science+Business Media, LLC 2007

Abstract Endothelial cells cover the inner surface of blood vessels and form the interface between the blood and the tissues. Endothelial cells are involved in regulating barrier function, which is maintained by the interendothelial cell contacts. These interendothelial cell contacts are established by the interaction of different molecules. The maintenance of the barrier requires an appropriate signalling between these molecules. Thus, a number of different signalling pathways are integrated within interendothelial contacts. Since endothelial cells are important in tissue-implant interactions (especially for stent materials) this study examines the expression pattern of different interendothelial contact molecules to determine the usefulness in the analysis of biocompatibility in vitro. The effects of different pro-inflammatory and toxic stimuli and contact of

human microvascular endothelial cells to metallic surfaces were examined for their impact on the pattern of interendothelial contact molecules. Striking modifications in the arrangement of these molecules were induced and the mode of modification was dependent on the tested compound. Thus, examining the pattern of expression of specific interendothelial contact molecules in vitro may be useful for testing the endothelial cell compatibility of biomaterials and their corrosion products.

Introduction

Vascular endothelial cells (EC) line the inner surface of all blood vessels. They form the interface between the circulating blood components and the surrounding tissues and are involved in the regulation of the blood-tissue barrier. EC take part in maintaining the homeostatic balance by the release or retention of different vasoactive factors respectively [1]. Due to their localisation, EC are among the first cells subjected to dysfunctions within the vascular system. There is a risk for toxin-induced impairment of EC and specific signals such as bacterial-induced pro-inflammatory reactions may affect EC and thus the balance within the vascular system. Such an imbalance may eventually lead to the loss of a regulated barrier function [2].

Interendothelial contacts are crucial for the maintenance of this barrier function. In most endothelia a specific arrangement of ultrastructural-identifiable formations can be found: i.e. tight junctions (*Zonulae occludentes*) and adherens junctions (*Zonulae adhaerentes*). In the maintenance of a regulated barrier function different tight junction molecules (e.g. occludin, ZO-1), adherens junction molecules (e.g. VE-cadherin) and CD31 (PECAM-1/platelet

K. Peters · R. E. Unger · S. Stumpf · J. Schäfer · R. Tsaryk · C. J. Kirkpatrick
Institute of Pathology, Johannes Gutenberg-University, Langenbeckstr. 1, 55101 Mainz, Germany

K. Peters (✉)
Department of Cell Biology, Junior Research Group, University of Rostock, Schillingallee 69, 18057 Rostock, Germany
e-mail: kirsten.peters@med.uni-rostock.de

B. Hoffmann · G. Ziegler
Friedrich-Baur-Forschungsinstitut für Biomaterialien, Universität Bayreuth, Ludwig-Thoma-Str. 36c, 95440 Bayreuth, Germany

E. Eisenbarth · J. Brems
Lehrstuhl für Metallische Werkstoffe, Universität des Saarlandes, 66041 Saarbrücken, Germany

G. Ziegler
BioCer EntwicklungsGmbH, Ludwig-Thoma-Str. 36c, 95447 Bayreuth, Germany

endothelial cell adhesion molecule) interact with each other [3]. F-actin is also involved in the endothelial barrier since the above mentioned junction molecules have a direct or indirect connection to the actin-cytoskeleton [4].

Interendothelial contacts are sites of intense signal transduction. This is indicated by the multitude of phosphatases and kinases located at the cell boundaries [5]. During inflammation, the interendothelial junctions are subjected to drastic changes, including the redistribution of CD31, VE-cadherin and the so-called peripheral actin ring. This redistribution leads to an increased permeability of the vessel wall which facilitates diapedesis of leukocytes (transmigration of leukocytes across the endothelial lining into interstitial fluid). It is suggested that these modifications of interendothelial contacts occur simultaneously by active contraction and passive disassembly [3].

EC are important in implant-tissue-interaction. EC are involved in inflammation by the expression of pro-inflammatory factors and are crucial for the process of blood vessel formation (called angiogenesis) [6]. Thus, EC have influence on wound healing after implantation and long-term implant stability. Furthermore, the re-endothelialization of the vessel wall after insertion of a vascular prosthesis (stent) is aimed at reducing the risk of thrombosis and restenosis. Thus, the maintenance of the full range of EC-functions (integrity of the cell layer, regulated proliferation, and angiogenesis potential) is a critical aspect in implant biocompatibility. EC *in vitro* maintain a number of different features that their counterparts express *in vivo*. Thus, EC *in vitro* can be used as a model system suitable for the examination of physiological and pathophysiological situations [7].

In this study we tested the suitability of the analysis of interendothelial contact molecules for assessment of EC-compatibility of materials. Therefore, the distribution pattern of different interendothelial contact molecules was analysed. Furthermore, the effects of biological pro-inflammatory factors (tumour necrosis factor- α /TNF α , lipopolysaccharide/LPS), toxic compounds (Co²⁺) and the direct contact with metallic implant materials (commercially pure titanium/cpTi and Co28Cr6Mo) were analysed to determine their effect on the interendothelial contacts.

Materials and methods

Materials

All chemicals, enzymes, antibiotics and biological factors were, if not indicated otherwise, supplied by Sigma (Germany). Cell culture plastics were from Becton Dickinson, TPP and Greiner (Germany).

Cell culture

Human dermal microvascular EC (HDMEC) were isolated from juvenile foreskin as described previously [8]. Before reaching confluency (average 3–5 days) HDMEC were separated from the miscellaneous cultures (containing EC and other cell types) by immunomagnetic isolation using CD31-Dynabeads (DynaL Biotech, Germany) according to the manufacturer's instructions. Cultivation of isolated HDMEC was with Endothelial Basal Medium MV (PromoCell, Germany) containing 15% heat-inactivated fetal calf serum (FCS), basic fibroblast growth factor (bFGF, 2.5 ng/mL), sodium-heparin (10 μ g/mL), 100 U/mL penicillin und 100 μ g/mL streptomycin (humidified atmosphere, 37 °C, 5% CO₂). All experiments were performed with cells in passage 3 or 4.

Time lapse video microscopy

HDMEC cultures (controls and CoCl₂-treated) were cultivated in a microscopic incubation chamber (supplied with an air/5% CO₂-mixture) in a humidified atmosphere for 24 or 48 h. Microscopic pictures were acquired with an inverted microscope (Leica, DM IRBE, Germany) and a DX30 camera (Kappa, Germany). The avi videos were generated with the software Kappa Image Base-Time (Kappa, Germany).

Immunofluorescence

HDMEC were seeded onto fibronectin-coated chamber slides (LabTek II CC2, Nunc, Germany). After reaching confluence (ca. 48 h after seeding) cells were exposed for a further 24 h under the specific cell culture conditions (e.g. 300 U/mL TNF α , 10 μ g/mL LPS, 0,7 mM CoCl₂). Afterwards the cells were fixed with buffered paraformaldehyde solution (3.7%, 15 min, room temperature). The detection of VE-cadherin and CD31 was by monoclonal antibodies from mice (VE-cadherin: BD Transduction Laboratories, Germany; CD31: Cymbus Biotechnology, UK). The AlexaFluor 488-labelled goat-anti-mouse-antibody (Molecular Probes, Germany) was used as secondary antibody. ZO-1 detection was by a polyclonal rabbit-antibody (Zymed/Invitrogen, Germany). Detection was performed by using the secondary AlexaFluor488-labeled donkey-anti-rabbit-antibody (Molecular Probes, Germany). F-actin staining was with AlexaFluor594-conjugated phalloidin (Molecular Probes, Germany). Nuclei were stained by Hoechst 33342 (1 μ g/mL). The stained samples were covered with fluorescence-mounting medium (Gel-Mount, Biomedica Corp/Natutec, Germany). Fluorescence

images were acquired with an epifluorescence microscope (DMRD, Leica) by using a digital camera (DC 300F, Leica).

Cytotoxicity

Cytotoxicity testing was carried out using the dye AlamarBlue™ (BioSource, Germany). The detection is based on the reduction of AlamarBlue™ by reduction equivalents (e.g. NADH etc.) produced during cellular metabolism. Overall the amount of reduction equivalents produced is proportional to cellular viability [9]. The reduction of AlamarBlue™ was fluorimetrically analysed after 30 min (Ex 560/Em 600 nm).

Preparation of metallic samples

The metal discs ($\varnothing = 15$ mm) were ground by repeated steps with abrasive paper of successively smaller granularity (60–1200), followed by polishing with a diamond paste and finally with a Al_2O_3 -suspension. The surface qualities of the polished discs were controlled microscopically. Surface roughness (R_a) was determined by white light interferometry. The average roughness of the samples was between 10 and 12 nm. Afterwards the discs were cleaned by sequential treatment with water, acetone, ethanol and water followed by autoclaving.

For the “direct contact” tests HDMEC were seeded on polished cpTi-(Titanium grade 2, HWN Titan GmbH, Germany) and Co28Cr6Mo-surfaces (cast alloy, Eska Implants GmbH, Germany) and cultivated for 48 h. Afterwards the cells were fixed and fluorescently stained for the above-mentioned interendothelial contact molecules.

Statistical analysis

The AlamarBlue™ assay was repeated four times (with threefold determination each) and the results are presented as means \pm standard deviation (SD). Statistical analysis was carried out using Excel 2003. Variance was analysed with the *F*-test. Differences between the means were analysed by the *t*-test ($p < 0.01$).

Results

Most vascular EC in vivo possess a typical appearance, the so-called cobblestone phenotype, which is characterized by

a polygonal shape. This polygonal shape is also exhibited in vitro and can be demonstrated by the detection of the CD31: In confluent HDMEC cultures CD31 was distributed within the intercellular contacts as a continuous, often laminar and jagged band which reflected the polygonality of the cells (Fig. 1a). The adherens junction-molecule VE-cadherin showed a similar distribution (Fig. 1b). However, the VE-cadherin band was narrower than that of CD31. The tight junction-molecule ZO-1 was displayed as a fine line within the cell contacts by immunofluorescence (Fig. 1c). Confluent layers of HDMEC showed the F-actin-cytoskeleton primarily at the cell periphery (Fig. 1d); often dominant actin-strands were detectable in parallel at the cell borders (arrowheads).

The pro-inflammatory stimulation of EC by $TNF\alpha$ and LPS led to drastic changes of the above-mentioned molecules: $TNF\alpha$ -stimulation induced a redistribution of CD31 (reduced in the intercellular contacts, partially spotted CD31-distribution over the whole cell area) (Fig. 1e). In contrast LPS-stimulation just led to the reduction of CD31 within the interendothelial contacts (Fig. 1i). Also the distribution of VE-cadherin was changed after pro-inflammatory stimulation; with both stimuli, $TNF\alpha$ and LPS, leading to a massive reduction of VE-cadherin within the interendothelial contacts (Fig. 1f— $TNF\alpha$, Fig. 1j—LPS). The remaining VE-cadherin appeared as a fine line that was more erratic compared to the controls. Furthermore, ZO-1 was drastically reduced within the intercellular contacts (Fig. 1g— $TNF\alpha$, Fig. 1k—LPS). For both molecules, VE-cadherin and ZO-1 the effects were more pronounced by LPS-stimulation. In non-stimulated HDMEC the F-actin was displayed as a peripheral ring (Fig. 1d). However, after pro-inflammatory stimulation cytoplasm-spanning F-actin fibrils were observed which have been referred to as ‘stress fibres’ (Fig. 1h— $TNF\alpha$, Fig. 1l—LPS). In addition, the differences between the treatment with $TNF\alpha$ and LPS were pronounced, the stress fibres being more apparent after $TNF\alpha$ -treatment compared with LPS-treatment.

A toxic substance, the metal salt $CoCl_2$, was used to examine effects on these interendothelial contact molecules. The phenotype of HDMEC after $CoCl_2$ -treatment changed from the polygonal shape of the untreated control cultures (Fig. 2a) into a spindle shape with long extensions (Fig. 2b, 0.7 mM $CoCl_2$, 24 h, arrowheads: cellular extensions). The $CoCl_2$ -concentration utilized (0.7 mM) was not cytotoxic as shown by the AlamarBlue™-assay (indicating metabolic activity) within 24 h of treatment (Fig. 3). Only the treatment with a fourfold higher $CoCl_2$ -concentration (3 mM) led to a significant reduction of AlamarBlue™-fluorescence and thus indicated a toxic effect. Longer exposure times of 2–3 days led to cell death (data not shown).

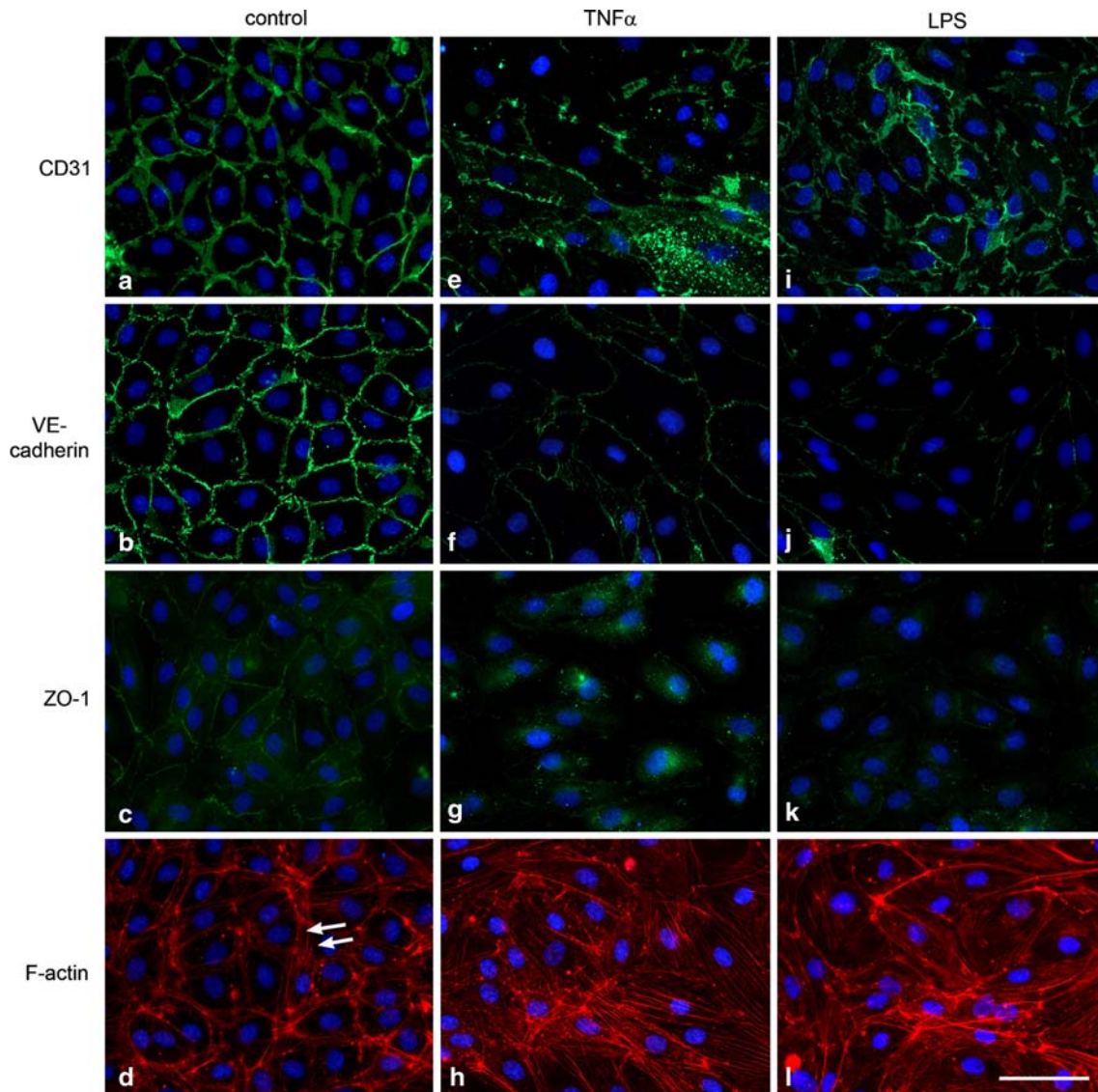


Fig. 1 Pattern of interendothelial contact molecules (CD31, VE-cadherin, ZO-1 and F-actin) in non-treated HDMEC in vitro (**a**: CD31, **b**: VE-cadherin, **c**: ZO-1, **d**: F-actin; *arrows*: parallel arrangement of F-actin filaments within the interendothelial contacts),

in TNF α -treated HDMEC (300 U/mL, 24 h; **e**: CD31, **f**: VE-cadherin, **g**: ZO-1, **h**: F-actin) and in LPS-treated HDMEC (1 μ g/mL, 24 h; **i**: CD31, **j**: VE-cadherin, **k**: ZO-1, **l**: F-actin; fluorescence microscopy, scale bar = 25 μ m)

However, the exposure of HDMEC to 0.7 mM CoCl₂ induced striking changes of CD31-expression within 24 h (Fig. 4). CD31-expression within the interendothelial contacts was reduced to a partial or complete disintegration of the continuous boundary (Fig. 4a). The expression of VE-cadherin within the intercellular contacts was also drastically reduced (Fig. 4b, diminution of the VE-cadherin ring pattern, reduction of fluorescence intensity in comparison to the untreated control). ZO-1 was hardly detectable after CoCl₂-treatment (Fig. 4c). Striking changes also occurred in F-actin distribution, with a multitude of cytoplasm-spanning F-actin fibres being detectable (Fig. 4d). Interestingly, the migratory activity of EC was increased by

CoCl₂-treatment compared to the untreated controls. Thus, especially during the first 24 h the cells showed a more pronounced floating within the cell layer (time lapse microscopy; video-link: untreated control: www.klinik.uni-mainz.de/pathologie/videos/2006_1, 0.7 mM CoCl₂-treated EC: www.klinik.uni-mainz.de/pathologie/videos/2006_2).

We also examined the effects that direct contact of HDMEC to metallic surfaces had on the expression pattern of the interendothelial contact molecules. We used mirror-polished discs of cpTi and Co28Cr6Mo. The adhesion of HDMEC on polished cpTi mostly led to a continuous marking of interendothelial contacts for CD31 (Fig. 5a), VE-cadherin (Fig. 5b) and ZO-1 (Fig. 5c) similar to the

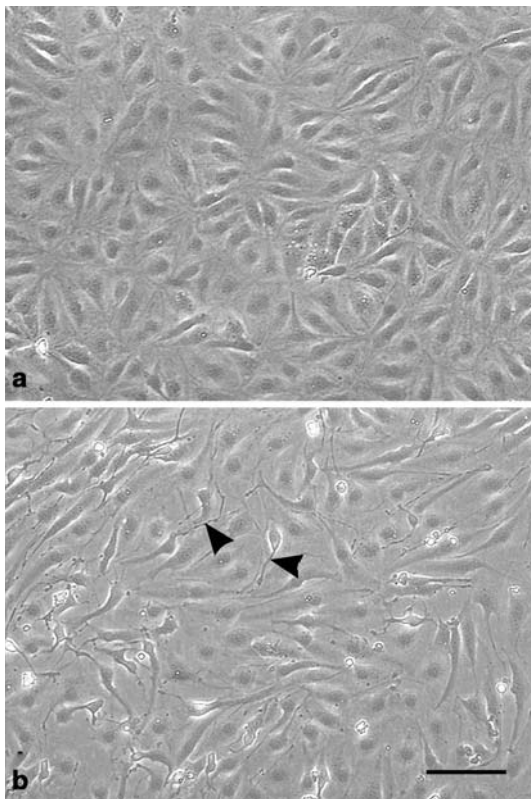


Fig. 2 (a) HDMEC in vitro (untreated control), (b) CoCl_2 -treated HDMEC (24 h, 0.7 mM, *arrowheads*: cellular extensions; phase contrast microscopy, scale bar = 50 μm)

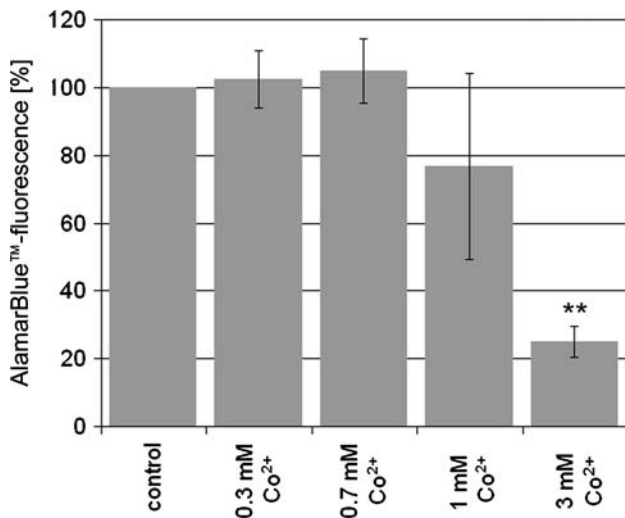


Fig. 3 AlamarBlue™-assay after 24 h exposure with different CoCl_2 -concentrations ($n = 4$; untreated control set as 100%; means \pm SD; ** $p < 0,01$)

untreated controls (HDMEC adhering on cell culture-suitable glass surfaces; Fig. 1a-d). However, the expression of VE-cadherin was faint compared to the controls. On cpTi-surfaces F-actin for the most part was detectable as peripheral actin rings. However, the rings were not as

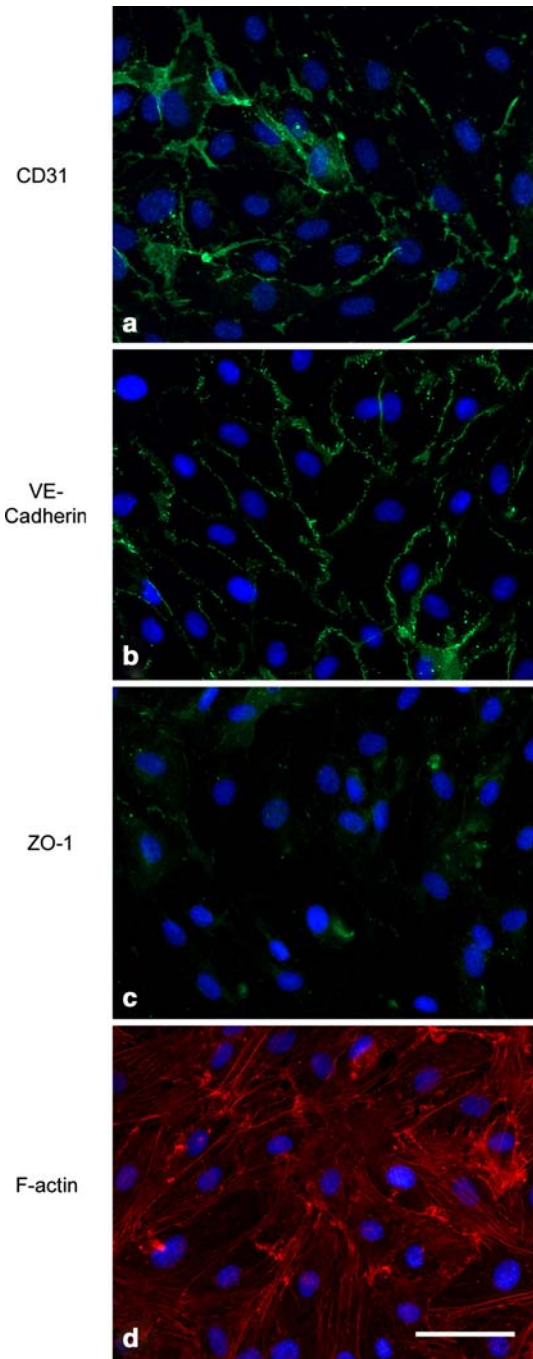
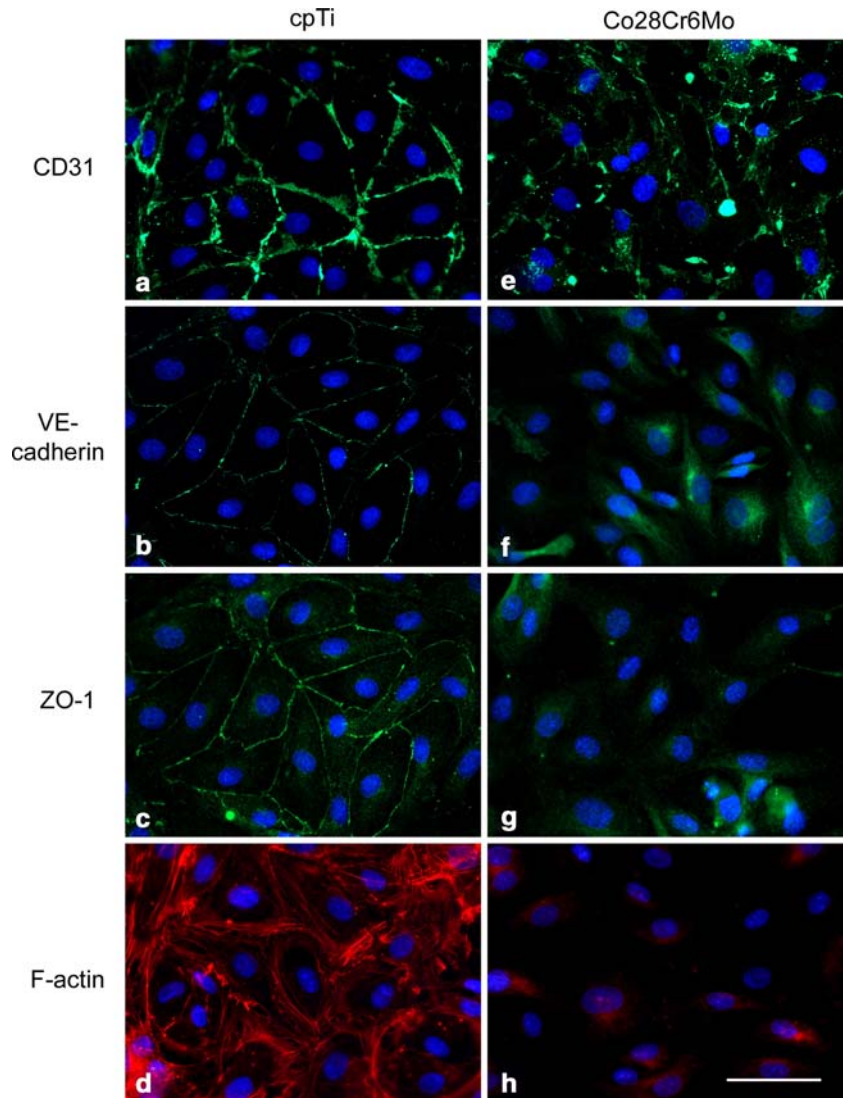


Fig. 4 Pattern of interendothelial cell contact molecules in HDMEC after 24 h exposure to 0.7 mM CoCl_2 . (a) CD31, (b) VE-cadherin, (c) ZO-1, (d) F-actin (fluorescence microscopy, scale bar = 25 μm)

pronounced and complete and a number of stress fibres were apparent (Fig. 5d). In contrast, the pattern of these molecules in HDMEC grown on Co28Cr6Mo-surfaces differed completely in comparison to cpTi. CD31-staining was extremely disrupted, scattered and distributed over the entire cell surface (Fig. 5e). Notably striking was the absence of the interendothelial contact distribution for

Fig. 5 Pattern of interendothelial cell contact molecules in HDMEC grown on mirror-polished cpTi (a: CD31, b: VE-cadherin, c: ZO-1, d: F-actin) and Co28Cr6Mo (e: CD31, f: VE-cadherin, g: ZO-1, h: F-actin; fluorescence microscopy, scale bar = 25 μ m)



VE-cadherin (Fig. 5f), ZO-1 (Fig. 5g) and F-actin (Fig. 5h) so that these molecules did not demonstrate any similarity to the usual staining pattern of the controls. Thus, neither VE-cadherin, ZO-1 nor F-actin showed the typical interendothelial pattern in HDMEC when grown on Co28Cr6Mo-surfaces.

Discussion

Numerous assays exist which examine cell viability or cytotoxicity, respectively, at different cellular levels (e.g. tetrazolium salt assays [10], calcein-AM-conversion [11] or the AlamarBlueTM assay [12] used in this study). For the detection of cell proliferation a number of assays are also available (e.g. BrdU- or 3H-thymidine-incorporation [13], Ki67-expression [14]). However, these tests only provide an indication of disruption of general cell functions such as

adhesion, metabolic activity, membrane integrity, and proliferation but provide no information about cell type-specific functions.

A fundamental cell type-specific function for non-activated EC is the integrity of the endothelial layer, which contributes to the physiological function of the endothelium [15]. Under inflammatory conditions, a disintegration of the endothelial layer occurs through the loosening of the interendothelial contacts leading to increased permeability of the endothelial layer. This increase in permeability facilitates leukocyte diapedesis and thus supports a pro-inflammatory state of the endothelium [2]. Furthermore, the loosening of interendothelial contacts leads to the exposure of subendothelial structures inducing an increased thrombogenicity [16]. Thus, an implanted material which affects the integrity of the endothelial layer, could provide a situation resulting in chronic inflammation, an increased thrombosis risk and an impaired blood circulation. The

direct corollary of coagulation activation would be especially important for vascular prosthesis (stents), since the development of thrombi could lead to occlusion of the blood vessel.

In this study different pro-inflammatory and toxic stimuli were examined for their effects on a number of characteristic molecular components of the interendothelial contact (i.e. CD31, VE-cadherin, ZO-1, and F-actin). We were able to show that the induction of a pro-inflammatory state, the exposure to toxic substances and the contact to a metallic surface (Co28Cr6Mo) influenced the pattern of the above-mentioned molecules. The type of change was, however, dependent on the stimulus: e.g. differences between the two pro-inflammatory factors, TNF α and LPS, became apparent (CD31- and F-actin-redistribution was more pronounced by TNF α stimulation; reduction of VE-cadherin and ZO-1 expression was higher with LPS). Since TNF α and LPS are pro-inflammatory stimuli which are recognized by different receptors (TNF α by TNF α -receptors [17] and LPS by toll-like receptor 4/TLR4 [18]), a difference in the degree and character of activation was expected.

The exposure of HDMEC to the metal salt CoCl₂, which has combined toxic and pro-inflammatory properties [19, 20], induced pattern changes of interendothelial contact molecules which deviated from the effects of the biological pro-inflammatory stimuli TNF α and LPS. Again, the influence on specific signalling processes (CoCl₂-induced activation of the NF κ B pathway [21] and CoCl₂-induced development of reactive oxygen species [22]) could be responsible for the pattern changes and the deviations from TNF α and LPS-induced effects.

Surprisingly, endothelial migratory activity was increased after treatment with CoCl₂. Whether this increased migratory activity was due to the dramatically changed phenotype under these conditions (EC became spindle-shaped with long extensions) is unclear. Since this phenotype is completely unusual for dying EC (normally they exhibit rounding-up and detachment) the results indicate that CoCl₂ may influence an as yet unknown signalling pathway in endothelial cells. Since the migratory activity of EC as well as the integrity of interendothelial contacts are regulated by numerous interacting molecules we can only speculate about the possible relationships. There is evidence that VCAM-1 (*vascular endothelial cell adhesion molecule-1*; which is also activated by CoCl₂ [23]) could be involved in intercellular contact signalling [24]. However, these results imply that the migratory activity of EC may not be a relevant indicator for biocompatibility when a toxic compound, such as Co²⁺, which eventually leads to cell death, first increases the migration of EC.

A significant difference was observed in the CoCl₂-induced effects on the pattern of interendothelial contact molecules compared to the cytotoxicity test Alamar-Blue™-assay. A marked change in the pattern of the interendothelial contacts after 24 h exposure was very obvious, whereas the cytotoxicity test did not show any similar indication of impairment of cell viability at the same concentration and time point (0.7 mM CoCl₂). Only higher CoCl₂-concentrations (≥ 3 mM) showed a significant reduction of cellular viability. Thus, the analysis of the interendothelial pattern indicated an impairment of endothelial function with much higher sensitivity than a conventional cytotoxicity assay.

The effects of direct contact of EC to metallic surfaces were striking. On polished cpTi-surfaces the pattern of interendothelial contact molecules was nearly unchanged compared with the untreated controls. In contrast, the pattern on Co28Cr6Mo-surfaces deviated completely. The cell layer was disintegrated and the pattern of all tested interendothelial molecules diverged from the controls. Interestingly, a recent animal study demonstrated that the CoCrMo-induced effect shown in vitro could be of relevance in vivo since in the tissues around CoCrMo implants, microvascular endothelial integrity was disrupted and massive edema occurred [25]. The trigger for these CoCrMo alloy-induced effects is as yet unknown. However, possible explanations could be the release of ions (e.g. Co²⁺) or specific physical characteristics of the metallic surface. These aspects are subject of a further study in which the analysis of current density, surface energy, wetting angle of contact, dielectric constant, and the superficial oxide film (by X-ray photoelectron spectroscopy/ESCA) is necessary.

In principal, the pattern changes were most obvious for CD31 and the F-actin cytoskeleton. One possible explanation for the distinctness of the effects may be found in the central physiological role of CD31 and F-actin. Whereas VE-cadherin and ZO-1 are indeed crucial for the regulation of endothelial permeability [26, 27], they are not active targets for leukocytes in the further steps involved in inflammation. In contrast, endothelial CD31 is an important adhesion molecule during the diapedesis of leukocytes [28] and the actin cytoskeleton integrates a multitude of signals of different classes of molecules (among them also the signals of VE-cadherin and occludin/ZO-1) [4]. Since the physiological reorganisation of interendothelial contacts is a result of active contraction and passive disintegration of the endothelial layer [3], the changes in the interendothelial phenotype additionally reflect the effects of pro-inflammatory factors as well as toxic substances in a highly sensitive manner.

Conclusions

Interendothelial cell contacts are formed by the interaction of different molecules and are sites of intensive signalling. In this study the phenotype of interendothelial contacts examined by the pattern of expression of different interendothelial contact molecules has been shown to be a sensitive and functional detection method for biocompatibility testing in vitro. Interestingly, the phenotypic changes differed depending on the compound tested, and this was possibly due to effects on different signalling pathways. Whereas conventional cytotoxicity tests often allow the throughput of high numbers, the depiction of the interendothelial contact pattern is not suitable for this type of screening procedure. However, although the detection of changes in the interendothelial contact patterns cannot substitute for conventional cytotoxicity tests, it does allow a detailed insight into the action and targets of cytotoxic compounds and is important for the understanding of how different compounds may exhibit unique effects on crucial endothelial cell functions. Moreover, we have shown this in vitro system to be much more sensitive than a general measure of cellular metabolic function.

Acknowledgement This work was supported by the German Research Foundation (Deutsche Forschungsgemeinschaft DFG, Priority Programme “Biosystem”, Ki 601/1-4). We would like to thank Susanne Barth for her excellent technical assistance.

References

1. D. B. CINES, E. S. POLLAK, C. A. BUCK, J. LOSCALZO, G. A. ZIMMERMAN, R. P. MCEVER, J. S. POBER, T. M. WICK, B. A. KONKLE, B. S. SCHWARTZ, E. S. BARNATHAN, K. R. MCCRAE, B. A. HUG, A. M. SCHMIDT and D. M. STERN, *Blood* **91** (1998) 3527
2. A. B. LENTSCH and P. A. WARD, *J. Pathol.* **190** (2000) 343
3. J. S. ALEXANDER and J. W. ELROD, *J. Anat.* **200** (2002) 561
4. H. J. SCHNITTLER, *Basic Res. Cardiol.* **93 Suppl 3** (1998) 30
5. Y. J. CHIU, K. KUSANO, T. N. THOMAS and K. FUJIWARA, *Endothelium* **11** (2004) 59
6. D. Y. SUH, *Ann. Clin. Lab. Sci.* **30** (2000) 227
7. C. J. KIRKPATRICK, M. OTTO, T. VAN KOOTEN, V. KRUMP, J. KRIEGSMANN and F. BITTINGER, *J. Mater. Sci. Mater. Med.* **10** (1999) 589
8. K. PETERS, H. SCHMIDT, R. E. UNGER, M. OTTO, G. KAMP and C. J. KIRKPATRICK, *Biomaterials* **23** (2002) 3413
9. K. KWACK and R. G. LYNCH, *Mol. Cells.* **10** (2000) 575
10. T. MOSMANN, *J. Immunol. Methods* **65** (1983) 55
11. X. M. WANG, P. I. TERASAKI, G. W. RANKIN Jr, D. CHIA, H. P. ZHONG and S. HARDY, *Hum. Immunol.* **37** (1993) 264
12. M. M. NOCIARI, A. SHALEV, P. BENIAS and C. RUSSO, *J. Immunol. Methods* **213** (1998) 157
13. T. L. LANIER, E. K. BERGER and P. I. EACHO, *Carcinogenesis* **10** (1989) 1341
14. T. G. VAN KOOTEN C. L. KLEIN and C. J. KIRKPATRICK, *J. Biomed. Mater. Res.* **52** (2000) 199
15. G. BAZZONI and E. DEJANA, *Physiol. Rev.* **84** (2004) 869
16. P. F. NIEVELSTEIN and P. G. DE GROOT, *Haemostasis* **18** (1988) 342
17. J. S. POBER, *Pathol. Biol. (Paris)* **46** (1998) 159
18. F. X. ZHANG, C. J. KIRSCHNING, R. MANCINELLI, X. P. XU, Y. JIN, E. FAURE, A. MANTOVANI, M. ROTHE, M. MUZIO and M. ARDITI, *J. Biol. Chem.* **274** (1999) 7611
19. C. J. KIRKPATRICK, S. BARTH, T. GERDES, V. KRUMPKONVALINKOVA and K. PETERS, *Mund Kiefer Gesichtschir.* **6** (2002) 183
20. K. PETERS, R. E. UNGER, S. BARTH, T. GERDES and C. J. KIRKPATRICK, *J. Mater. Sci. Mater. Med.* **12** (2001) 955
21. M. WAGNER, C. L. KLEIN, T. G. VAN KOOTEN and C. J. KIRKPATRICK, *J. Biomed. Mater. Res.* **42** (1998) 443
22. S. LEONARD, P. M. GANNETT, Y. ROJANASAKUL, D. SCHWEGLER-BERRY, V. CASTRANOVA, V. VALLYATHAN and X. SHI, *J. Inorg. Biochem.* **70** (1998) 239
23. M. WAGNER, C. L. KLEIN, H. KLEINERT, C. EUCHENHOFER, U. FORSTERMANN and C. J. KIRKPATRICK, *Pathobiology.* **65** (1997) 241
24. S. VAN WETERING, N. VAN DEN BERK, J. D. VAN BUUL, F. P. MUL, I. LOMMERSE, R. MOUS, J. P. TEN KLOOSTER, J. J. ZWAGINGA and P. L. HORDIJK, *Am. J. Physiol. Cell. Physiol.* **285** (2003) C343
25. C. N. KRAFT, B. BURIAN, O. DIEDRICH, J. GESSMANN, M. A. WIMMER and P. H. PENNEKAMP, *J. Biomed. Mater. Res. A.* **75** (2005) 31
26. F. BREVIARIO, L. CAVEDA, M. CORADA, I. MARTIN-PADURA, P. NAVARRO, J. GOLAY, M. INTRONA, D. GULINO, M. G. LAMPUGNANI and E. DEJANA, *Arterioscler. Thromb. Vasc. Biol.* **15** (1995) 1229
27. M. S. BLUM, E. TONINELLI, J. M. ANDERSON, M. S. BALDA, J. ZHOU, L. O'DONNELL, R. PARDI and J. R. BENDER, *Am. J. Physiol.* **273** (1997) H286
28. G. CEPINSKAS, J. SAVICKIENE, C. V. IONESCU and P. R. KVIETYS, *J. Cell Biol.* **161** (2003) 641